

Comment on “Physical and electronic structure and magnetism of Mn₂NiGa: Experiment and density-functional theory calculations”

S. R. Barman¹ and Aparna Chakrabarti²

¹UGC-DAE Consortium for Scientific Research, Khandwa Road, Indore 452001, India

²Raja Ramanna Centre for Advanced Technology, Indore 452013, India

(Received 13 August 2007; published 6 May 2008)

Recently, Liu *et al.* [Phys. Rev. B **74**, 054435 (2006)] published the electronic structure of Mn₂NiGa by using *ab initio* spin-polarized density functional theory. In the martensitic phase, they report a large decrease in Mn and Ni local magnetic moments to almost zero and a large increase in the density of states at the Fermi level. By total energy minimization, considering various possible starting Mn moment configurations, we show that the above mentioned results do not correspond to the minimum total energy solution. Our results are in agreement with the experimentally observed decrease in magnetization in the martensitic phase and the photoemission valence band spectrum, whereas the results of Liu *et al.* are in disagreement.

DOI: [10.1103/PhysRevB.77.176401](https://doi.org/10.1103/PhysRevB.77.176401)

PACS number(s): 75.50.Cc, 71.20.Lp, 64.70.K-, 71.15.-m

Ferromagnetic shape memory alloy (FSMA) materials are of current interest after the discovery of 10% magnetic field-induced strain in Ni-Mn-Ga.^{1,2} Mn₂NiGa is a newly discovered FSMA in the Ni-Mn-Ga family that exhibits about 4% shape memory effect.³ It has an L_{2_1} cubic structure in the austenitic phase and tetragonally distorts in the martensitic phase.³ Mn₂NiGa is a promising material for novel technological applications because its Curie temperature is high (588 K), while the martensitic start temperature (270 K) is close to room temperature.

Liu *et al.*⁴ recently performed both experimental and theoretical studies on Mn₂NiGa. The electronic structures of both cubic austenitic and tetragonal martensitic Mn₂NiGa were calculated by self-consistent full-potential linearized-augmented plane-wave (FPLAPW) method by using the experimental lattice constants. It was found that austenitic Mn₂NiGa shows ferrimagnetism due to antiparallel but unbalanced magnetic moments of Mn atoms at A and B sublattices with local magnetic moments of $-2.20\mu_B$ and $3.15\mu_B$ for Mn(A) and Mn(B), respectively. However, they found that in the martensitic phase, the magnetic moment of Mn(A) atoms decrease by 50% and Mn(B) and Ni moments are almost completely suppressed. Hence, they concluded that martensite Mn₂NiGa shows ferromagnetic coupling. A large change in the density of states (DOS), which is accompanied by a substantial increase at E_F , was reported in the martensitic phase.⁴

The differences between the calculated total energies (E_{tot}) as a function of lattice constants are small for the FSMA Heusler alloys. So, disagreements exist in literature even for Ni₂MnGa that is ferromagnetic and has been well studied.⁵⁻⁹ Mn₂NiGa is expected to have a more complicated magnetic structure than Ni₂MnGa because of the direct Mn-Mn interaction in Mn₂NiGa.¹⁰ In this work, we show that E_{tot} minimization should be performed with different starting Mn moments with parallel and antiparallel alignments. However, this was not reported in Ref. 4. The quenching of Mn and Ni local magnetic moments to almost zero in the martensitic phase⁴ is physically unexpected. Moreover, the conclusions in Ref. 4 do not agree with the large body of literature on related shape memory alloys, such as Ni₂MnGa, Ni₂MnAl, Ni-Ti, and Pd-Ti.⁵⁻¹⁵

The unusual theoretical results for Mn₂NiGa presented in Ref. 4 prompted us to perform a detailed electronic structure calculation by using FPLAPW method employing the WIEN97 code.¹⁶ A generalized gradient approximation (GGA) for the exchange correlation that accounts for the density gradients was used.¹⁷ The crystal structure is taken to be L_{2_1} , which is similar to that of Ni₂MnGa.^{3,18} As in Ref. 4, Mn(B) atoms occupy the same site as Mn atoms in Ni₂MnGa and Mn(A) are the additional Mn atoms. We call Mn(A) as MnI and Mn(B) as MnII to keep consistency of the notation used in our recently published work on Mn₂NiGa.¹⁹ An energy cutoff for the plane wave expansion of 16 Ry is used ($R_{MT}K_{\text{max}}=9$). The cutoff for charge density is $G_{\text{max}}=14$. The maximum l (l_{max}) for the radial expansion is 10 and for the nonspherical part, $l_{\text{max,ns}}=6$. The muffin-tin radii are Ni: 2.1364, Mn: 2.2799, and Ga: 2.1364 a.u. The number of k points for self-consistent field (SCF) cycles in the irreducible Brillouin zone is 256 and 484 in austenitic and martensitic phase, respectively. The convergence criterion for E_{tot} is 0.1 mRy, which implies that the accuracy of E_{tot} is ± 0.34 meV/atom. The charge convergence is set to 0.001. Some calculations have been performed with convergence criteria of 0.05 mRy in energy and 0.0005 in charge.

We have obtained the lowest energy magnetic state by performing the minimization of E_{tot} with various possible starting MnI and MnII magnetic moment combinations for three electrons in the Mn $3d$ $\kappa=-3$ state. κ is the relativistic quantum number given by $-s(j+1/2)$, where s is the spin quantum number and $j=l+s/2$.¹⁶ The maximum occupancy of the $\kappa=-3$ state is 6, i.e., 3 for each spin. The occupancy of the Mn $3d$ $\kappa=2$ state is kept unchanged with one electron each in majority- and minority-spin states. For the austenitic phase, the calculations have been performed with the experimental lattice constants.³ From the first four entries in Table I, we note that when MnI and MnII starting magnetic moments are antiparallel, irrespective of whether they are equal or unequal, the calculations converge to a ferrimagnetic state. This state has the minimum E_{tot} , which is taken to be 0 meV in the relative energy scale. For the martensitic phase (Table II), we find the similar trend that the SCF runs with antiparallel starting MnI and MnII moments converge to the lowest

TABLE I. Starting and converged Mn spin magnetic moments (the configuration, i.e., the occupancy in the majority- and minority-spin states in the starting Mn $3d \kappa=-3$ state is shown in parentheses, separated by a comma) and the corresponding converged total energies (E_{tot}) for the austenitic phase of Mn_2NiGa . The lowest E_{tot} is taken to be 0 meV/atom as a reference (for the first four rows E_{tot} varies at most by 0.03 meV/atom). The muffin-tin radii are 5% higher in this set of data compared to Table II and Ref. 19.

Starting Mn moment (μ_B) and spin configuration		Converged Mn moment (μ_B)		Converged E_{tot} (meV/atom)
MnI	MnII	MnI	MnII	Total
1 (2,1)	-1 (1,2)	2.65	-3.30	0
1 (2,1)	-3 (0,3)	2.65	-3.30	0
-1 (1,2)	3 (3,0)	-2.65	3.30	0
-3 (0,3)	3 (3,0)	-2.66	3.30	0
-1 (1,2)	-3 (0,3)	0.63	-3.03	75
3 (3,0)	3 (3,0)	2.83	3.07	159
-3 (0,3)	-1 (1,2)	-2.28	-1.53	178

E_{tot} (0 me V) and a ferrimagnetic solution is obtained. In all cases, the starting Ni moment is taken to be zero and it develops a small moment aligned along MnII after convergence. E_{tot} has been further minimized as a function of the lattice constants and we find that the martensitic phase is about 6.8 meV/atom lower in energy compared to the austenitic phase.¹⁹

In the austenitic phase, initial spin configurations, where MnI and MnII spins are parallel (equal or unequal), converge to either ferromagnetic or ferrimagnetic states but at different local minima with higher E_{tot} at 75, 159 and 178 meV/atom (Table I). Also in the martensitic phase (Table II), parallel starting MnI and MnII moments converge to a higher energy local minimum and a ferromagnetic solution is obtained. For example, the E_{tot} local minimum at about 171 meV/atom is obtained for starting moments of $3\mu_B$ each in parallel configuration, which converge to moment values of 2.58 and $2.83\mu_B$ for MnI and MnII, respectively. Interestingly, for starting MnI and MnII magnetic moments of $1\mu_B$ and $3\mu_B$,

respectively, we obtain the MnI moment to be small ($0.4\mu_B$), converging at a E_{tot} local minimum of 109 meV. This indicates that there might be local minima in the E_{tot} hyperspace where one Mn atom moment is small and this might have happened in Ref. 4. So, we performed calculations starting with the Mn moments reported for MnGaNiMn from Table I of Ref. 4. We find that E_{tot} converges to a local minimum at 194 meV/atom (see Table II last but one row) and the converged MnI, MnII, and Ni moments are $1.38\mu_B$, $-0.12\mu_B$, and $0.02\mu_B$, respectively, which are quite similar to those in Ref. 4. A calculation with $3\mu_B$ and $0\mu_B$ Mn starting moments converges to 180 meV/atom with $2.48\mu_B$, $-0.19\mu_B$, and $0.03\mu_B$ on MnI, MnII, and Ni, respectively (last row, Table II). Thus, quenching of MnII and Ni moment is possible for certain starting Mn moment configurations. However, it is clear that this is an artifact of the calculation caused by convergence to a local minimum. Table I and II clearly show that it is indeed possible to converge to different local minima at a considerably higher energy and obtain com-

TABLE II. Starting and converged Mn spin magnetic moments (the configuration, i.e., the occupancy in the majority- and minority-spin states in the starting Mn $3d \kappa=-3$ state is shown in parentheses separated by a comma) and the corresponding total energies (E_{tot}) for the martensitic phase of Mn_2NiGa . The lowest E_{tot} is taken to be 0 meV/atom as the reference (for the first four rows E_{tot} varies at most by 0.18 meV/atom).

Starting Mn moment (μ_B) and spin configuration		Converged Mn moment (μ_B)		Converged E_{tot} (meV/atom)
MnI	MnII	MnI	MnII	Total
-3 (0,3)	3 (3,0)	-2.19	2.90	0
3 (3,0)	-1 (1,2)	2.19	-2.89	0
-3 (0,3)	1 (2,1)	-2.18	2.88	0
1 (2,1)	-3 (0,3)	2.17	-2.89	0
1 (2,1)	3 (3,0)	0.40	2.39	109
1 (2,1)	1 (2,1)	0.88	1.95	119
-3 (0,3)	-1 (1,2)	-1.44	-1.43	128
3 (3,0)	3 (3,0)	2.58	2.83	171
1.38 (2.19,0.81)	0.01 (1.505,1.495)	1.38	-0.12	194
3 (3,0)	0 (1.5,1.5)	2.48	-0.19	180

TABLE III. Interatomic distances in the austenitic and martensitic phases of Mn_2NiGa in Å.

Atom pairs	Austenitic	Martensitic
Ni-MnI	2.925	2.701
Ni-MnII	2.533	2.549
MnI-MnII	2.533	2.549

pletely different Mn moments. In Ref. 4, no calculation with different starting Mn moments is reported and the starting Mn moments that were used are also not mentioned. Tables I and II show that it is likely that Liu *et al.*⁴ performed their calculation with a particular starting Mn moment combination that has converged to a local minimum.

Lattice constant optimization was not performed in Ref. 4 but this turns out to be an unlikely reason for the disagreement with our results since the difference between optimized¹⁹ and experimental³ lattice constants is small (2%). Besides, our calculations with experimental and optimized lattice constants yield similar magnetic moments. Furthermore, since the calculations in Ref. 4 were done by using local density approximation (LDA), we have calculated the magnetic moments by using LDA for the lattice constant optimized structure. The LDA local moments for MnI, MnII, Ni, and Ga in the martensitic phase are $-1.95\mu_B$, $2.73\mu_B$, $0.27\mu_B$, and $0.01\mu_B$, respectively. These are not very different from the GGA values for the same structure: $-2.21\mu_B$, $2.91\mu_B$, $0.27\mu_B$, and $0.01\mu_B$ for MnI, MnII, Ni, and Ga, respectively.¹⁹ Mn moments are somewhat smaller in LDA but the total moment is somewhat higher in LDA ($1.06\mu_B$). So, the use of LDA is not the reason for the disagreement of our results with Ref. 4. Furthermore, we have performed the calculations by using all the stated parameters (e.g., number of k points, muffin-tin radii, and plane-wave cutoff) in Ref. 4 that are different from our values. We find that the differences in these parameter values are not the reason for the disagreement either.

Direct interaction between incomplete d shells generally favors antiferromagnetic alignment.^{20,21} The exchange pair interaction as a function of distance was calculated for Mn in a Heisenberg-type model. Antiferromagnetic coupling at short interatomic distances, such as 2.82 Å, was found, which becomes ferromagnetic at larger distances.²⁰ The short distance of 2.533 Å between MnI and MnII (Table III) in the austenitic phase was used by Liu *et al.*⁴ to explain the anti-parallel coupling of MnI and MnII moments. However, it should be noted that in the martensitic phase, the MnI-MnII [i.e., Mn(A)-Mn(B) in Ref. 4], distance only slightly increases to 2.549 Å (Table III). So, the above argument should also be valid for the martensitic phase.

According to Ref. 4, if I ($=E_x/\mu_B$) is similar to J ($=0.87$), intra-atomic exchange will prevail. Table I of Ref. 4 shows that $I=0.95$ and 0.89 for Mn(A) and Mn(B), respectively, in the austenitic phase, while it is 0.94 for Mn(A) in the martensitic phase. Thus, $I \approx J$ for both phases. If $I \approx J$ in the martensitic phase, there is no reason why intra-atomic interaction should be completely suppressed. Thus, there is an inconsistency in their argument to explain the large

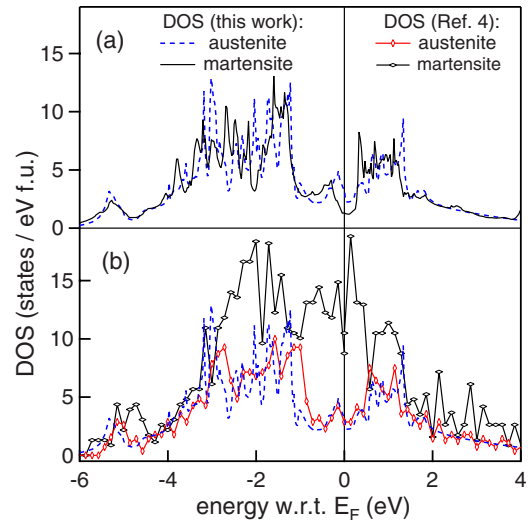


FIG. 1. (Color online) Comparison of the total DOSs of Mn_2NiGa for the austenitic and the martensitic phases from (a) this work and (b) Ref. 4.

change in Mn magnetic moments. To justify their result, Liu *et al.*⁴ compared the DOS in their Figs. 3 and 5 and concluded that the Mn $3d$ bands are much more localized in energy for austenite than martensite.

It is noteworthy that although c/a is 1.25 in the martensitic phase, the increase in c is compensated by the decrease in a and b so that interatomic distances change by a small amount between the two phases (Table III). Such small changes in interatomic distances is unlikely to result in a drastic change in hybridization leading to quenching MnII and Ni moments in the martensitic phase.⁴

In Fig. 1(a), we compare the DOS of the austenitic and martensitic phases of Mn_2NiGa . The DOS shows a small but significant shift of the peak at -0.1 eV near E_F in the martensitic phase.¹⁹ However, for both phases, the main peak appears at a similar energy and the DOS are not substantially different. In Fig. 1(b), we show the DOS of Mn_2NiGa obtained by adding the published majority- and minority-spin DOS from Fig. 5 of Ref. 4. Our calculated austenitic phase DOS agrees fairly well with that of Ref. 4 [Fig. 1(b)]. In stark contrast, the martensitic phase DOS shows a large difference. A large increase in the DOS at E_F is clearly visible. The intensity at E_F is comparable to the peak in the DOS that occurs around -2 eV. Such a drastic change in the DOS between the austenitic and martensitic phases has not been observed in any other shape memory alloy.^{5-9,11}

As is expected, the integrated total number of occupied states between -6 eV and E_F is similar between the austenitic (24.89 states/eV f.u.) and martensitic (24.85 states/eV f.u.) phases in our case. In contrast, the integrated total number of occupied states is about double in the martensitic phase compared to the austenitic phase, although the unit of the DOS is the same in both Figs. 3 and 5 of Ref. 4. This is obviously not correct since the total number of available electrons in the valence band (VB) cannot change so much between the two phases.

The magnetic moments reported in Ref. 4 are inconsistent with their own magnetization data.^{3,4} It is reported that the

martensitic phase saturation magnetic moment is about 9% lower than the austenitic phase: $1.21\mu_B/\text{f.u.}$ (28.28 emu/g) and $1.29\mu_B/\text{f.u.}$ (30.3 emu/g) in martensitic and austenitic phases, respectively.³ This qualitative trend should be an important test for the theory. However, Liu *et al.*⁴ reported that the total theoretical magnetic moment of the martensitic phase ($1.41\mu_B$) is larger than the austenitic phase ($1.28\mu_B$). This contradiction is admitted by them. The total moment for the martensitic phase we obtained is $1.01\mu_B/\text{f.u.}$, while the austenitic phase total moment is $1.12\mu_B/\text{f.u.}$ Thus, the martensitic phase moment is 10% less than the austenitic phase, which is in good agreement with the trend in experimental magnetization data.³

The theoretical total moment in the martensitic phase we calculated is smaller than the experimental value of $1.4\mu_B$ at 5 K reported by Liu *et al.*⁴ Such disagreement between experiment and theory might arise because of different reasons: In the case of Mn_2NiGa , magnetization could be highly composition dependent because it is given by the difference between two large moments (MnI and MnII). For example, if only 5% MnI moment is aligned parallel to MnII, the resulting total moment (including the Ni moments) will increase by about 23%. Even a slight Ni excess will result in regions in the specimen that would resemble a Ni_2MnGa -like environment where the Mn moments are aligned parallel, giving rise to a higher total moment. Such situations can arise due to compositional inhomogeneity, gradient in composition, and antisite disorder. These issues were not addressed in Ref. 4. Another possible reason for the disagreement could be that in reality the magnetic structure of Mn_2NiGa is more complicated than ferrimagnetic. For example, the higher experimental magnetic moment can be explained if MnI moments are canted with respect to the MnII and Ni moments. Possible occurrence of spiral moments was studied by Enkovaara *et al.*²² for Ni_2MnGa . However, such calculations are

beyond the scope of the present work and were also not considered in Ref. 4.

The large difference between DOSs, as shown in Fig. 1, impelled us to perform photoemission spectroscopy. We show in Ref. 19 that the experimental valence band spectrum is in good agreement with the theoretically calculated VB. On the contrary, using the partial DOS from Ref. 4, the calculated VB is clearly different from the photoemission valence band spectrum.¹⁹ As can be expected from the total DOS in Fig. 1(b), the intensity near E_F is even higher than the main peak and the main peak position at -2 eV also does not agree with the experiment (-1.4 eV). This clearly shows that the DOS reported in Ref. 4 does not agree with the experimental photoemission data.

In conclusion, we show that for Mn_2NiGa , total energy calculations with various possible starting magnetic moments of the inequivalent MnI and MnII atoms are required to obtain the minimum energy magnetic state. Our results demonstrate that it is possible to reach local minima in total energy depending on the starting Mn moments. For both the austenitic and the martensitic phases, we show that the ground state is ferrimagnetic. This is in disagreement with Ref. 4, which reported the martensitic phase to be ferromagnetic with quenching of MnII [Mn(B) in their notation] and Ni magnetic moments. This can be related to the possible convergence to a local minimum in Ref. 4. Despite a small change in the nearest neighbor distances, the drastic variation in Mn and Ni moments and the DOS in the martensitic phase obtained in Ref. 4 are physically unexplainable and do not agree with our calculations and the available experimental data.

P. Chaddah, V. C. Sahni, A. Gupta, S. M. Oak, and K. Horn are thanked for the encouragement. Funding for this work from Ramanna Research Grant and Max Planck Partner Group Project is acknowledged.

¹S. J. Murray, M. Marioni, S. M. Allen, R. C. O'Handley, and T. A. Lograsso, *Appl. Phys. Lett.* **77**, 886 (2000).

²A. Sozinov, A. A. Likhachev, N. Lanska, and K. Ullakko, *Appl. Phys. Lett.* **80**, 1746 (2002).

³G. D. Liu, J. L. Chen, Z. H. Liu, X. F. Dai, G. H. Wu, B. Zhang, and X. X. Zhang, *Appl. Phys. Lett.* **87**, 262504 (2005).

⁴G. D. Liu, X. F. Dai, S. Y. Yu, Z. Y. Zhu, J. L. Chen, G. H. Wu, H. Zhu, and J. Q. Xiao, *Phys. Rev. B* **74**, 054435 (2006).

⁵S. Fujii, S. Ishida, and S. Asano, *J. Phys. Soc. Jpn.* **58**, 3657 (1989).

⁶V. V. Godlevsky and K. M. Rabe, *Phys. Rev. B* **63**, 134407 (2001).

⁷A. Ayuela, J. Enkovaara, and R. M. Nieminen, *J. Phys.: Condens. Matter* **14**, 5325 (2002).

⁸A. Chakrabarti, C. Biswas, S. Banik, R. S. Dhaka, A. K. Shukla, and S. R. Barman, *Phys. Rev. B* **72**, 073103 (2005).

⁹S. R. Barman, S. Banik, and A. Chakrabarti, *Phys. Rev. B* **72**, 184410 (2005).

¹⁰J. Enkovaara, O. Heczko, A. Ayuela, and R. M. Nieminen, *Phys. Rev. B* **67**, 212405 (2003).

¹¹G. Bihlmayer, R. Eibler, and A. Neckel, *J. Phys.: Condens. Matter* **5**, 5083 (1993).

¹²P. J. Brown, A. Y. Bargawi, J. Crangle, K.-U. Neumann, and K. R. A. Ziebeck, *J. Phys.: Condens. Matter* **11**, 4715 (1999).

¹³Z. Islam, D. Haskel, J. C. Lang, G. Srager, Y. Lee, B. N. Harmon, A. I. Goldman, D. L. Schlagel, and T. A. Lograsso, *J. Magn. Magn. Mater.* **303**, 20 (2006).

¹⁴B. L. Ahuja, B. K. Sharma, S. Mathur, N. L. Heda, M. Itou, A. Andrejczuk, Y. Sakurai, Aparna Chakrabarti, S. Banik, A. M. Awasthi, and S. R. Barman, *Phys. Rev. B* **75**, 134403 (2007); C. Biswas, R. Rawat, and S. R. Barman, *Appl. Phys. Lett.* **86**, 202508 (2005).

¹⁵S. Banik, Aparna Chakrabarti, U. Kumar, P. K. Mukhopadhyay, A. M. Awasthi, R. Ranjan, J. Schneider, B. L. Ahuja, and S. R. Barman, *Phys. Rev. B* **74**, 085110 (2006).

¹⁶P. Blaha, K. Schwartz, and J. Luitz, *WIEN97* (Karlheinz Schwarz, Technical Universität Wien, Austria, 1999).

¹⁷J. P. Perdew, K. Burke, and M. Ernzerhof, *Phys. Rev. Lett.* **77**, 3865 (1996).

¹⁸S. Banik, R. Ranjan, A. Chakrabarti, S. Bhardwaj, N. P. Lalla, A.

- M. Awasthi, V. Sathe, D. M. Phase, P. K. Mukhopadhyay, D. Pandey, and S. R. Barman, *Phys. Rev. B* **75**, 104107 (2007); R. Ranjan, S. Banik, S. R. Barman, U. Kumar, P. K. Mukhopadhyay, and D. Pandey, *ibid.* **74**, 224443 (2006).
- ¹⁹S. R. Barman, S. Banik, A. K. Shukla, C. Kamal, and A. Chakrabarti, *Europhys. Lett.* **80**, 57002 (2007).
- ²⁰D. Hobbs, J. Hafner, and D. Spisak, *Phys. Rev. B* **68**, 014407 (2003).
- ²¹C. Zener, *Phys. Rev.* **81**, 440 (1951).
- ²²J. Enkovaara, A. Ayuela, J. Jalkanen, L. Nordström, and R. M. Nieminen, *Phys. Rev. B* **67**, 054417 (2003).